ELSEVIER

S0032-3861(96)00185-1

Polymer Vol. 37 No. 16, pp. 3675–3682, 1996

0032-3861/96/$15.00+0.00

Mechanism and kinetics of polymerization of a dicyanate ester resin photocatalysed by an organometallic compound

Heping Liu and Graeme A. George*

School of Chemistry and CIDC, Queensland University of Technology, GPO Box 2434, Brisbane 4001, Australia

(Received 28 November 1995; revised 4 January 1996)

The kinetics of the thermal polymerization of the dicyanate ester Arocy B-10 (4,4′-dicyanato-2,2′-diphenylpropane), following irradiation in the presence of the catalyst tricarbonyl cyclopentadienyl manganese ($CpMn(CO)_3$), has been investigated using d.s.c. and *FT*i.r. It was found that the network developed a higher T_g at lower extents of conversion than observed in uncatalysed thermal polymerization. The rate of the decrease of cyanate concentration was described by a first-order dependence on the active catalyst concentration and the cyanate concentration. The activation energies were calculated for the different irradiated systems, and they decreased with the increase of the irradiation time. Cyanate with a pre-made catalyst system which aimed to simulate the directly irradiated system were also studied, and the kinetic parameters were determined. A mechanism of cyclotrimerization is proposed based on the kinetic data as well as the *FT*i.r. spectra from a model study. This involves the photo-substitution of the carbonyl groups in the catalyst by the cyanate groups (L) during irradiation to form complexes $CpMn(CO)_{3-x}L_x$ which are suggested to produce the active catalyst by thermal decomposition. Copyright © 1996 Elsevier Science Ltd.

(Keywords: dicyanate esters, organometallic compounds; network polymerization kinetics)

INTRODUCTION

The cyanate esters such as 4,4′-dicyanato-2,2′-diphenylpropane (**1**) are of growing interest because of their advantages in electrical and mechanical properties over the other presently used resins in applications such as the printed circuit board and the structural composite industry[1]. This is available commercially as the 98% pure compound (Arocy B-10, Ciba-Geigy) as a crystalline solid.

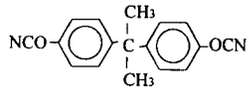

Arocy B-10 (4,4′-dicyanato-2,2′-diphenylpropane)

The main reaction of the polymerization of the cyanates is the formation of the triazine ring[2] (*Scheme 1*), which can be catalysed by active hydrogen compounds like phenol or amine, or by transition metal complexes such as cobalt naphthenate or copper acetylacetonate[1,3,4].

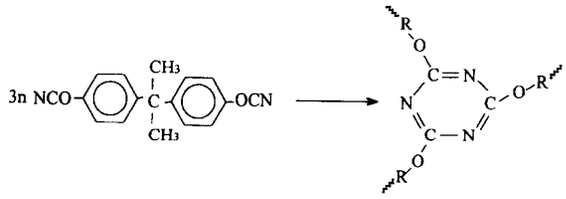

Scheme 1 Triazine ring formation (R is the bisphenol moiety)

* To whom correspondence should be addressed

There have been a number of reports of the kinetics and mechanism of the thermal polymerization reaction. Without added catalysts, the reaction is supposed to be catalysed by impurities including moisture and residual phenol from synthesis[5]. The kinetics were described by a second-order[6,7] or a third-order[8,9] autocatalytic model. With added transition metal catalysts, the reaction occurs via the gathering of cyanate ester by transition metal (*Scheme 2*)[4] and is co-catalysed by active hydrogen, but there is no evidence reported for direct coordination between metal and cyanate functional groups resulting in a stable intermediate. The overall reaction rate was reported to display a first-order dependence on the initial metal concentration and

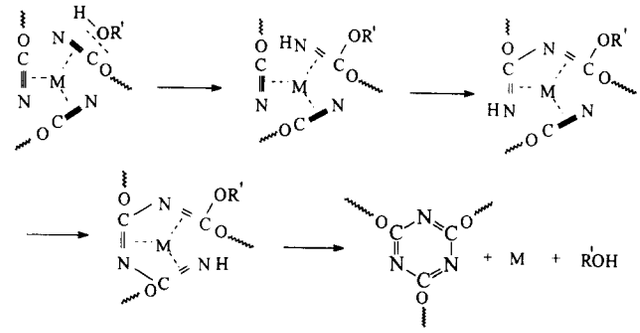

Scheme 2 Catalysed thermal trimerisation. M is a metal cation and R′OH represents a compound with active hydrogen

first[10] or second[6] order dependence on the cyanate concentration[6].

There are also a few reports[11–14] about using organometallic compounds as catalysts which exhibit better solubility in the cyanates with some being photocurable. However, there have been no detailed studies of these systems published. This work aims to understand the mechanism and kinetics of photocuring, which is important not only for a better understanding of the cure process, but also for optimization of the conditions for fabrication of materials from cyanate esters.

EXPERIMENTAL

Materials

The Arocy B-10, bisphenol A cyanate ester used in this study (4,4′-dicyanato-2,2′-diphenylpropane) was obtained from Hi-Tek Polymer and recrystallized again from hexane. This produced needle-like white crystals with a melting point of 80°C. The tricarbonyl cyclopentadienyl manganese, $CpMn(CO)_3$, was purchased from Aldrich and used as obtained (elemental analysis result: C 47%; H 2.5%; O 21%). Benzene was of spectroscopic quality.

Sample preparation

The Arocy B-10 + 1 mol% $CpMn(CO)_3$ sample was prepared by mixing 6.65 mg (0.0325 mmol) of $CpMn(CO)_3$ with 453 mg (3.25 mmol OCN group) of B10 after briefly melting them at 90°C and stirring thoroughly. It was then stored in a desiccator.

Irradiated samples were prepared by melting the above mixture at 90°C first and immediately irradiating for different times. The samples remained in the liquid state during irradiation, but the i.r. spectrum indicated no detectable polymerization happened during this stage. The irradiation source was broad-band u.v.–visible radiation from a 150 W high pressure mercury lamp. The lamp intensity was measured to be approximately 0.15 mW cm^{-2} using an Oriel pyroelectric detector. The irradiated samples were wrapped with aluminium foil and stored in a desiccator for subsequent use.

A model study was performed by using a higher catalyst concentration to form photo-adducts with the cyanate ester; 90.3 mg (0.650 mmol OCN group) of B-10 was dissolved in 50 ml of benzene in a 100 ml round-bottomed flask which was equipped with a magnetic stir bar[15]. After deoxygenizing with nitrogen for 15 min, 66.0 mg (0.325 mmol) of $CpMn(CO)_3$ was added and the mixture was irradiated at room temperature under nitrogen for 30 min using a high pressure mercury lamp which was placed about 140 mm from the flask horizontally. After finishing irradiation, the sediment was filtered and washed with benzene and dried in vacuum. The *FT*i.r. spectrum of the dried product (which was a mixture) was then obtained using a Perkin-Elmer 1600 spectrophotometer. Because of the difficulty in separating the photoproducts due to the decomposition in solution, the catalytic properties of the mixture were studied. Inductively coupled plasma emission analysis was used to measure an average Mn concentration of 1.73 mol kg^{-1}.

A series of B-10 samples with various added amounts of the above product were made by simple grinding, with catalyst concentrations of 4.1×10^{-4}, 8.1×10^{-4} and 1.24×10^{-3} mol Mn mol^{-1} OCN.

D.s.c. and FT*i.r. kinetic studies*

The d.s.c. experiments were performed using a Setaram DSC92 under a nitrogen atmosphere. The samples were tightly sealed in aluminium pans. The dynamic scans were run from 30 to 380°C at a rate of 10°C min^{-1}. The isothermal scans were performed by ramping from 30°C to the isothermal temperature at a rate of 30°C min^{-1}, then holding at this temperature until there was no further change of heat flow. The samples were then quenched to room temperature and run from 30 to 370°C at 10°C min^{-1} to obtain the residual heat and glass transition temperature T_g, which was taken at the half heat capacity change point.

The amount of heat released up to time t(ΔH_t) was determined by integrating the rate of heat flow *versus* time curve of the isothermal run from time 0 to time t, and the total heat released (ΔH_T) of the reaction was obtained by adding the total isothermal heat released and the residual heat from the subsequent d.s.c. scan until no further heat flow occurred. So the degree of conversion (α) is calculated by

$$\alpha = \Delta H_t / \Delta H_T \quad (1)$$

The reaction rate was calculated by the expression[16]:

$$d\alpha/dt = (dQ/dt)/\Delta H_T \quad (2)$$

where dQ/dt is the rate of heat flow, which can be obtained from the isothermal d.s.c. measurement.

The *FT*i.r. studies were performed using a Perkin-Elmer 2000 spectrophotometer equipped with an electrical heating jacket (P/N 20707) for the sample and an automatic temperature controller (P/N 20140). The irradiated samples were cast from acetone on KBr cells and heated at 70°C briefly to remove the residual solvent. The sample cells were then secured in the sample holder, which allowed for *in situ* analysis of the curing reaction. Spectra were taken at intervals of 60 s for 1 to 2 h. The cyanate concentration was expressed in terms of relative peak area of CN stretch at 2236 and 2272 cm^{-1} using the C–H stretch at 2970 cm^{-1} as the reference peak. The degree of conversion (α) was calculated as

$$\alpha = 1 - A_t/A_0 \quad (3)$$

where A_t is the relative cyanate concentration at time t and A_0 is the initial relative cyanate concentration obtained from the respective peak areas.

RESULTS AND DISCUSSION

U.v. irradiation

The dynamic d.s.c. scan curves of the irradiated and non-irradiated B-10 samples containing $CpMn(CO)_3$ are plotted in *Figure 1*. It is very obvious from the shift of the exotherm maximum that the 120-s irradiated sample cured at a much lower temperature than the non-irradiated one. The pure B-10 system was also checked with irradiation and without irradiation, and there was negligible difference between the two curves which indicated that there was no photocatalysis of the reaction without the Mn compound. It was also found that there was very little difference in the d.s.c. curves between the pure B-10 and the unirradiated B-10 + $CpMn(CO)_3$ system, which implied no catalysis of the polymerization by the $CpMn(CO)_3$ compound without u.v. irradiation.

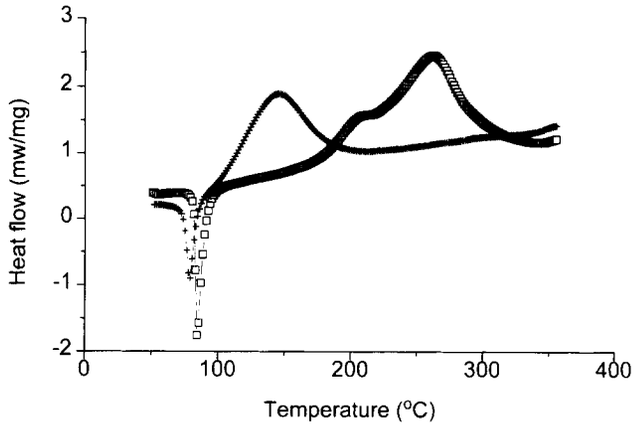

Figure 1 D.s.c. dynamic scans of different irradiated B-10 + 1% $CpMn(CO)_3$ samples: (+) 120 s irradiated; (□) non-irradiated

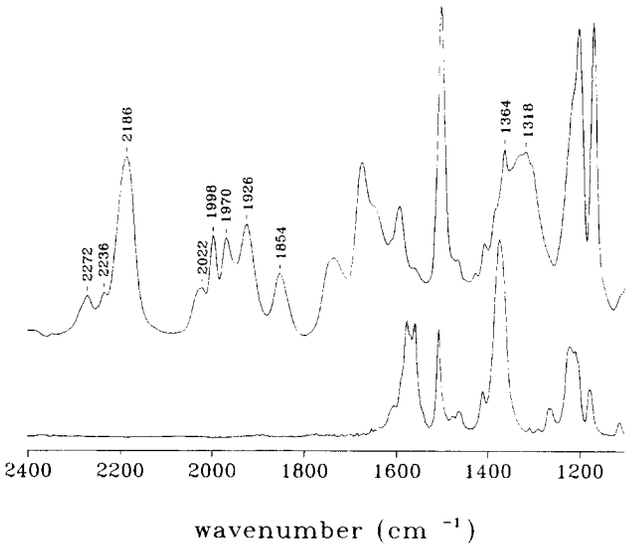

Figure 2 *FT*i.r. spectra of the model study. Upper spectrum: B-10 + $CpMn(CO)_3$ after irradiation, with a OCN/Mn molar ratio of 2:1; lower spectrum: fully cured B-10 without catalyst

Table 1 Assignment of the main i.r. bands of the spectra of the photochemical reaction products of B-10 and $CpMn(CO)_3$ with a OCN/Mn molar ratio of 2:1

Wavenumber (cm^{-1})	Assignment
2272, 2236	Simple C≡N stretch
2186	Coordinated C≡N stretch[17,20]
2022, 1926	C≡O stretch ($CpMn(CO)_3$)[20]
1998, 1970	C≡O stretch ($CpMn(ROCN)(CO)_2$)[21]
1854	C≡O stretch ($CpMn(CO)(ROCN)_2$)[21]
1564	Trimer ring stretch[1]
1364	C–O and trimer ring stretch[1]

From the fact that with no u.v. irradiation there was no polymerization for either the pure B-10 or the B-10 + $CpMn(CO)_3$ system at the same temperatures at which the irradiated systems polymerized, it can be suggested that some species of active catalyst formed after irradiation. A change from almost colourless to green or to deep brown, depending on the irradiation time, was observed, indicating the formation of new species. However, the low concentration of the newly formed species in the presence of monomer prevented their detailed analysis.

Model study of active photocatalyst formation

To investigate the species formed after the irradiation, a model system was used which contained higher catalyst concentration (OCN/Mn molar ratio 2:1) than the practical system used for the kinetic studies. This was necessary in order to determine if there was interaction between the cyanate functional group and the metal cation by spectroscopic methods. The reaction was conducted in solution to ensure uniform irradiation at low temperature, because otherwise the polymerization would occur during irradiation at the temperature above the melting point of B-10. During irradiation, the solution colour changed from bright yellow to blue, then a deep blue solid precipitated. The *FT*i.r. spectrum of the solid is given in *Figure 2*, and the assignments of the main bands of the spectrum are listed in *Table 1*. The spectrum of fully cured B-10 cyanate ester without catalyst is also shown in order that the bands due to complexation between the catalyst and cyanate ester may be readily seen.

As can be seen from *Figure 2*, besides the original CN stretching bands (2272 and 2236 cm^{-1}), a new band appears which is centred at 2186 cm^{-1}. This can be assigned as the coordinated C≡N stretch. The decrease of the frequency indicates the η^2-type coordination[17] of CN with the Mn atom and considerable $d - \pi^*$ backbonding from metal to ligand, because otherwise the frequency would increase if the coordination was simply N-bonded[18,19].

The appearance of new CO stretching bands (1998 and 1970 cm^{-1}) implies the existence of the monosubstituted product $CpMn(CO)_2L$[20,21] and the 1854 cm^{-1} CO stretching band indicates the formation of a bisubstituted product $CpMn(CO)L_2$. A blank experiment with only $CpMn(CO)_3$ and benzene was repeated under the same conditions and neither a colour change nor formation of precipitate occurred. After recovery, the catalyst showed no new CO stretching band, which confirms that the ligand, L, is the cyanate functional group.

However, if the two C≡N groups simply coordinated with the Mn in the bisubstituted product $CpMn(CO)(ROCN)_2$, the corresponding C≡N stretching bands, which are supposed to be different from the monosubstituted product, should be seen. Since there was no evidence for these bands, the bisubstituted product may have the form of **2** instead of the form of **3**[22].

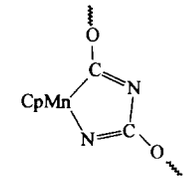

2

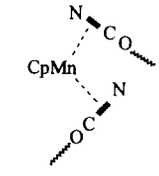

3

The appearance of the 1364 cm^{-1} band indicates the formation of trimer ring at the high catalyst concentration in this model system, and the broad band with a peak at 1318 cm^{-1} may be due to the trisubstituted product $CpMn(ROCN)_3$.

In summary, coordination between the cyanate functional group and the Mn is clearly supported. However, to determine the exact substituted form needs more evidence. An attempt using electrospray mass spectroscopy to obtain the individual product mass has failed to give any useful results. This may be due to the lack of

sensitivity of the product or the low solubility in the solvents (methanol and acetonitrile) which must be used. The difficulty in separating the mixture was mainly caused by the facile decomposition of the products in solution. However, even if the monosubstituted product were the only complex formed after the irradiation in solution, it is also possible that bisubstituted or trisubstituted complexes could form in the bulk state where the cyanate concentration and the local OCN/Mn ratio were much higher than in the solution.

These results are consistent with the well-known photochemistry of $CpMn(CO)_3$[20], which is dominated by CO photosubstitution, and the substitution of the η^5-Cp ring is not a primary photochemical event. Though similar compounds to $CpMn(NCOR)_3$ have not been reported, compounds like $CpFe(CNPh)_3Cl$ and $CpFe(CNPhCH_3)_3PF_6$ have been synthesized and characterized[23]. Since Mn(I) and Fe(II) both have d^6 electron structure and they are adjacent in the periodic table, their coordination behaviour should be very similar. The activity of this product mixture was investigated by d.s.c. and was found to be an active catalyst as described in the following section.

Network formation

To investigate further the kinetics and mechanism of this photocatalysed polymerization, d.s.c. isothermal experiments on different irradiated systems were performed. In addition, to assess the active catalyst concentration, systems with various concentrations of the above pre-made solid catalyst were also studied.

Figure 3 is a plot of degree of conversion (from equation (1)) *versus* polymerization time for the different irradiated samples cured at the same temperature of 120°C. It is noted that the reaction rate declines well before complete conversion. This is observed in most isothermal network polymerizations and corresponds to the diffusion controlled region at the cure temperature[9]. However, in this case the reaction reached a different limiting conversion which increased with time of irradiation. This is unusual, because if the network formed was the same, the reaction should proceed to the same extent, which is determined by the reaction temperature, until the reaction becomes diffusion controlled. To verify the value of the degree of conversion obtained from d.s.c. isothermal data, a comparison with those from the *FT*i.r. is plotted in *Figure 4*, and it is seen that the two analytical methods are consistent within experimental error.

The T_g values measured by d.s.c. after the cure are shown in *Tables 2* and *3*. It is noted that the difference between the cure temperature and the T_g of the resin decreases as the irradiation time increases. For the pre-made catalyst system the difference is much lower than for the irradiated system. However, all the T_g values were lower than those of the cure temperature T_c. This indicates that the onset of the diffusion control occurred in the rubbery state, before vitrification occurred. This agrees with the behaviour of another cyanate system studied (Arocy RTX366)[9], but different from that of aromatic epoxy/aromatic amine systems where diffusion control began at vitrification[24,25]. The T_g–conversion relationships for the irradiated, unirradiated and pre-made catalyst systems are shown in *Figure 5*. This master curve may be compared with that obtained by Georjon *et al.*[8] by the thermal cure of B-10 over the temperature range 150–250°C. They fitted their data to a modified DiBenedetto equation:

$$T_g = T_{g0} + \frac{(T_{gM} - T_{g0})(\Delta C_{pM}/\Delta C_{p0})\alpha'}{(1-\alpha) + (\Delta C_{pM}/\Delta C_{p0})\alpha'} \quad (4)$$

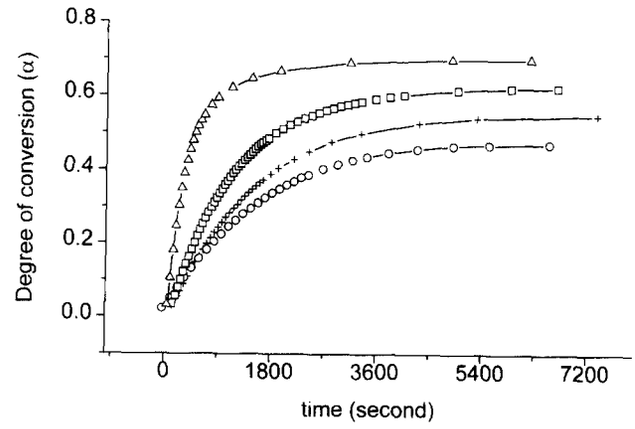

Figure 3 Plot of degree of conversion vs. time of different irradiated B-10 + 1% $CpMn(CO)_3$ samples cured at 120°C: (○) 15 s irradiation; (+) 30 s irradiation; (□) 60 s irradiation; (△) 120 s irradiation

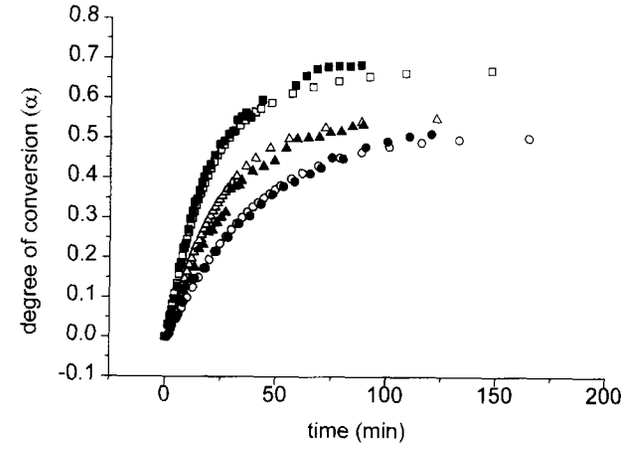

Figure 4 Comparison of degree of conversion values obtained from d.s.c. (open symbols) and *FT*i.r. (solid symbols) data for the 30 s irradiated B-10 + 1% $CpMn(CO)_3$ samples cured at different temperatures (■□) 130°C; (▲△) 120°C; (●○) 110°C

Table 2 The glass transition temperatures of the Arocy B-10 cured by $CpMn(CO)_3$ after different times of irradiation

Irradiation time (s)	Isothermal temperature (°C)	T_g (°C)	Degree of conversion (α)
0	210	153	0.84
0	220	202	0.91
0	230	219	0.96
15	120	53	0.52
15	130	60	0.55
15	135	64	0.57
15	140	87	0.66
30	110	55	0.50
30	120	60	0.55
30	130	90	0.67
60	100	<30	0.50
60	110	70	0.53
60	120	76	0.62
60	130	86	0.63
120	120	111	0.71

Table 3 The glass transition temperature of Arocy B-10 cured by the pre-made catalyst

Pre-made catalyst concentration (10^{-4} mol Mn mol^{-1} OCN)	Isothermal temperature (°C)	T_g (°C)	Degree of conversion (α)
4.1	120	96	0.65
4.1	130	107	0.70
4.1	140	116	0.74
8.1	120	99	0.66
8.1	130	111	0.71
8.1	140	122	0.75
12.4	105	80	0.60
12.4	110	82	0.62
12.4	120	101	0.71

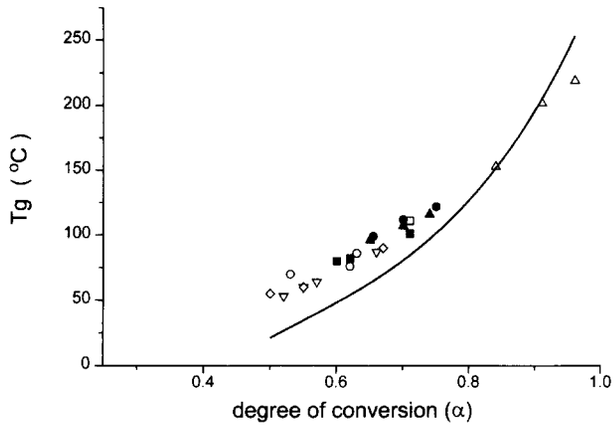

Figure 5 Master curve of T_g as a function of extent of conversion (measured by d.s.c.) for curing of different irradiated B-10 + 1% $CpMn(CO)_3$ systems (open symbols) and B-10 + pre-made catalyst systems (solid symbols). The curve for equation (4), which is a modified DiBenedetto equation for the uncatalysed thermal cure of B-10[6], is shown for comparison (solid line)

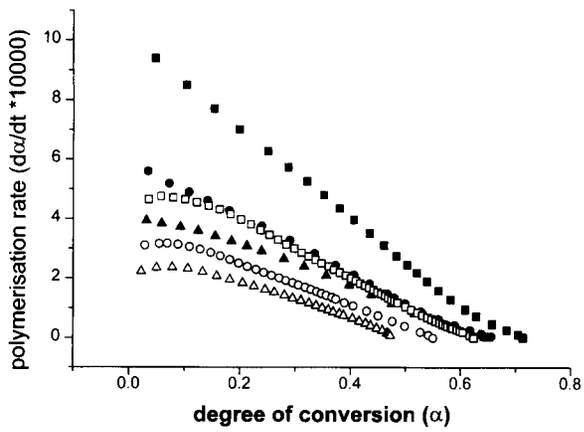

Figure 6 Polymerization rate dependence of B-10 on the active catalyst concentration for different irradiated B-10 + 1% $CpMn(CO)_3$ systems (open symbols) and B-10 + pre-made catalyst systems (solid symbols) cured at 120°C: (△) 15 s irradiation; (○) 30 s irradiation; (□) 60 s irradiation; (▲) 4.1×10^{-4} mol Mn mol^{-1} OCN; (●) 8.1×10^{-4} mol Mn mol^{-1} OCN; (■) 1.24×10^{-3} mol Mn mol^{-1} OCN

where account is taken of the topological limitation to achieving 100% cure by replacing $T_{g\infty}$ by T_{gM}, the maximum T_g achieved at the ultimate extent of conversion; α' is then the ratio of extent of conversion to the ultimate achieved. In their studies T_{gM} was 243°C at $\alpha = 0.95$ and when this is used the plot shown in *Figure 5*

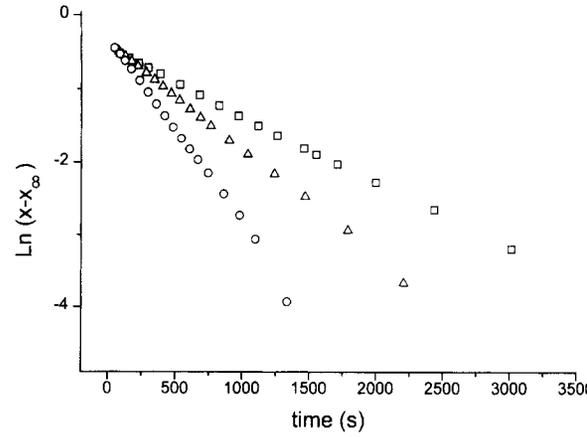

Figure 7 Plot of logarithm of modified cyanate fraction, $\ln(x - x_\infty)$, vs. polymerization time for the B-10 + 810 ppm Mn pre-made catalyst system cured at different temperatures: (□) 120°C; (△) 130°C; (○) 140°C

is obtained. It is seen that the agreement with our data for the thermal polymerization (high α) is good, but there is substantial deviation at low conversion, which corresponds to the photocatalysed polymerization. The network in all cases has attained a T_g higher than predicted from the uncatalysed thermal polymerization studies.

This suggests a fundamental difference between the two networks which is probably related to the differences in mechanism. For example, the catalysed system may have achieved greater cyclotrimerization for the same amount of consumption of cyanate.

This would also indicate that gelation may have occurred at a lower extent of conversion. Mean-field theory has predicted a gel point at 50% conversion[26], but it has been frequently reported that this gel point for cyanate ester resins occurs between 58 and 64% conversion[8,27], corresponding to a T_g of 50°C[8]. In this photocatalysed system the lowest T_g observed was 50°C and from *Figure 5* this corresponds to 50% conversion as predicted from mean-field theory. The reasons for the discrepancy in the thermal polymerization has been widely discussed and one suggestion has been the steric limitations on reactivity[28]. The observation of gelation at $\alpha = 0.5$ when curing under an inert atmosphere[8] has led to moisture effects on the cure reaction being suggested. We are presently undertaking dynamic rheological studies of gel formation in the photocatalysed system to explore further the gel time–conversion dependence and the comparison with the prediction of mean-field theory to resolve this problem.

Kinetic analysis

Figure 6 presents an analysis of the d.s.c. data in which the instantaneous reaction rate (from equation (2)) is plotted against the extent of conversion.

It may be seen from *Figure 6* that there was an increase in reaction rate, at a given temperature, with an increase in either the irradiation time or an increase in the pre-made catalyst concentration. This indicates that the active catalyst concentration increased with the irradiation time.

To determine the reaction order with respect to the cyanate concentration, $\ln(x - x_\infty)$, where x is the ratio of the unreacted cyanate concentration to the initial value and x_∞ is a constant, was plotted against reaction time (*Figure 7*). They all showed a linear relationship until the

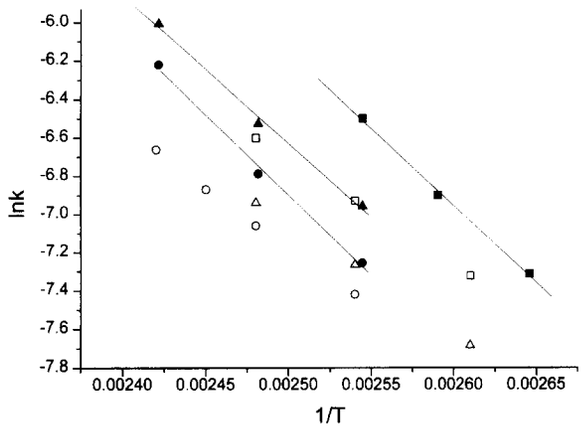

Figure 8 Arrhenius plot for different irradiated B-10 + 1% $CpMn(CO)_3$ systems (open symbols) and B-10 + pre-made catalyst systems (solid symbols): (○) 15 s irradiation; (△) 30 s irradiation; (□) 60 s irradiation; (●) 4.1×10^{-4} mol Mn mol^{-1} OCN; (▲) 8.1×10^{-4} mol Mn mol^{-1} OCN; (■) 1.24×10^{-3} mol Mn mol^{-1} OCN

Table 4 Activation energies for the cure of B-10 + 1% $CpMn(CO)_3$ system after different time of irradiation and for the cure of B-10 with added different concentrations of pre-made catalyst

Irradiation time (s) or pre-made catalyst concentration (mol Mn mol^{-1} OCN)	Activation energy value (kJ mol^{-1})
15 s	52 ± 1
30 s	48 ± 1
60 s	46 ± 1
4.1×10^{-4} mol Mn mol^{-1} OCN	70 ± 5
8.1×10^{-4} mol Mn mol^{-1} OCN	64 ± 4
1.24×10^{-3} mol Mn mol^{-1} OCN	67 ± 2

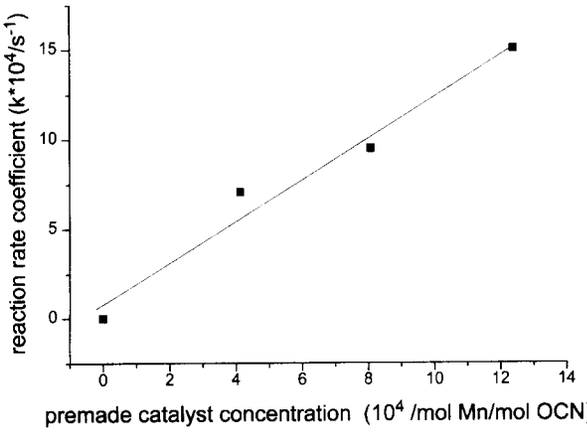

Figure 9 Plot of polymerization rate coefficient vs. added active catalyst concentration cured at 120°C

extent of conversion of 0.65 for the pre-made catalyst systems and 0.50–0.63 for the directly irradiated systems, corresponding to the onset of diffusion control. The x_∞ values were 0.35 ± 0.02 for the pre-made catalyst systems and 0.37–0.50 for the directly irradiated systems. The x_∞ values can be considered as the unreacted cyanate fraction when diffusion control occurred; thus, the $x - x_\infty$ stands for the relative cyanate fraction which undertook a similar path within the kinetically controlled region, while the x_∞ part would react under diffusion controlled conditions and is limited by the high viscosity in the rubbery state. The reaction is then first order in this 'reactive' concentration of cyanate $(x - x_\infty)$.

The reaction rate coefficient can be obtained from the slope of the line, and the results for the different temperatures and different systems are presented in *Figure 8* as Arrhenius plots.

The activation energies were then obtained and the results are summarized in *Table 4*. For the pre-made catalyst systems the consistent values of the activation energy within experimental error indicate the same mechanism for the different concentrations. For the directly irradiated systems, there is a trend of decline of activation energies with increase of the irradiation time. Considering this decrease and the fact that the activation energies for the directly irradiated systems are lower than that of the pre-made catalyst systems, it may be suggested that in the different irradiated systems, the composition of different forms of the active catalyst, which could be the mono-, bi- or tri-substituted product of the compound $CpMn(CO)_3$ as discussed before, would change with the irradiation time. It may also be suggested that, in the directly irradiated systems, more of the most active catalyst would be produced than in the pre-made catalyst, because the activation energies are lower. This most active catalyst could be the trisubstituted product of $CpMn(CO)_3$, considering that the OCN/Mn molar ratio in the directly irradiated systems was much higher than that from which the pre-made catalyst was produced.

From *Figure 7*, the kinetic model can be written as

$$-dx/dt = k'(x - x_\infty)$$

The constant k' will also include a factor for the active catalyst concentration:

$$k' = k''[\text{cat}]^m$$

To determine the value of m, the reaction rate coefficients at the same temperature were plotted against added pre-made catalyst concentration (*Figure 9*). The linear line through the origin yields the value for m of unity. So the total kinetic equation should have the following form:

$$-dx/dt = k[\text{cat}](x - x_\infty)$$

where [cat] is the added pre-made catalyst concentration. For the directly irradiated systems, because of the complexity of the relationship between active catalyst concentration and irradiation time, it is difficult to obtain a similar plot, but it is supposed that, for each catalytic species, the kinetic relation would have a similar form.

Proposed mechanism of photocatalysis of cyclotrimerization

Several mechanisms have been suggested for the transition metal catalysed polymerization of cyanate esters such as *Scheme 2*[4], discussed in the Introduction, and *Scheme 3*[10] below. However, neither appears to be applicable to the photocatalysed ring formation reported here.

In *Scheme 2*, the catalysts discussed were transition metal carboxylates or acetylacetonates where coordination between the metal and oxygen was strong and the key factor in breaking the cyanate triple bond was a compound with an active hydrogen as a co-catalyst,

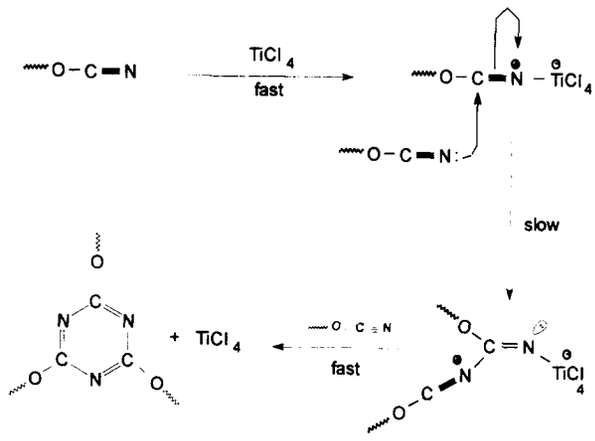

Scheme 3 N-bonded complex intermediate in $GiCl_4$ catalysed trimerisation

whilst the metal gathered cyanate groups into close proximity for ring formation. In this case, it would not be expected that irradiation would accelerate the reaction significantly if the metal oxidation state was unchanged. Since it was found that irradiation reduced the onset temperature of the photocatalysed cure of cyanates dramatically, the mechanism of this system would seem to be different. Unlike carboxylates or acetylacetonates in the thermal catalysts in *Scheme 2*, the coordinated carbonyl groups in this photocatalyst can be easily displaced by cyanate groups under irradiation. In addition, there is evidence that coordination between cyanates and metal cation was π-bonded, where a shift to lower wavenumber of the CN stretching band in the *FT*i.r. spectrum was observed, rather than N-bonded as in *Scheme 3* where the shift was to higher wavenumber. Based on the above discussion and references[22] about the mechanism of the photocatalysed pyridine ring formation, and in combination with the experimental results presented, a proposed mechanism for the photocatalysed polymerization of cyanates is outlined in *Scheme 4* and discussed below.

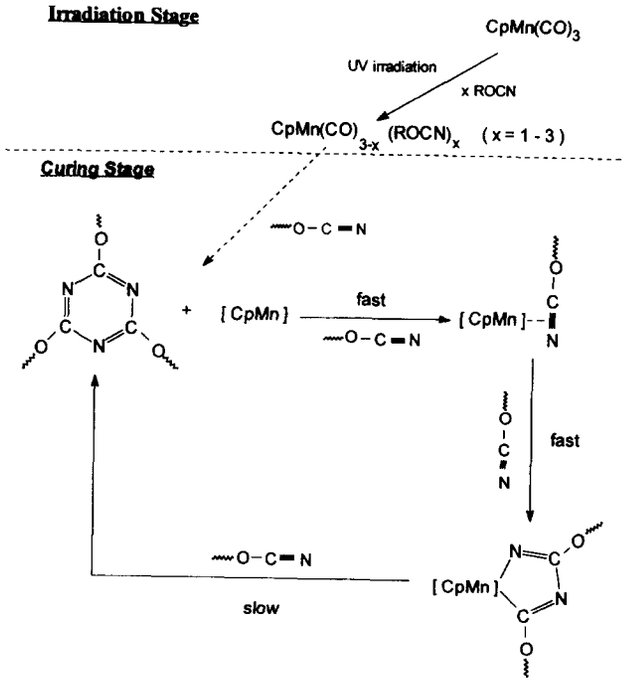

Scheme 4 A proposed mechanism for the photocatalysed polymerization of cyanates

At the irradiation stage, part or all of the CO groups may be replaced by between one and three cyanate groups, then, at the thermal curing stage, the remaining carbonyls will be replaced by the cyanate functional groups and eventually the triazine ring formed. A coordinatively unsaturated species CpMn (or CpMn(CO)) will be released in this step, which is expected to be very active and will combine with other cyanates quickly. This process will be repeated, resulting in a large number of catalytic cycles leading to network formation. However, as discussed before in the kinetic study section, several mechanisms could proceed due to the complexity of catalyst composition.

According to this mechanism, assuming that the last step of addition of the third cyanate group and formation of the triazine ring is the rate-determining step, then the following equations can be written:

$$\mathrm{CpMn} + \mathrm{ROCN} \xrightarrow{k_1} \mathrm{CpMn(ROCN)} \quad (5)$$

$$\mathrm{CpMn(ROCN)} + \mathrm{ROCN} \xrightarrow{k_2} \mathrm{CpMn(ROCN)_2} \quad (6)$$

$$\mathrm{CpMn(ROCN)_2} + \mathrm{ROCN} \xrightarrow{k_3} \mathrm{CpMn} + \mathrm{Triazine} \quad (7)$$

So

$$-\mathrm{d[ROCN]}/\mathrm{d}t = k_3[\mathrm{CpMn(ROCN)_2}][\mathrm{ROCN}] \quad (8)$$

From equations (5) and (6) assuming a steady state concentration of the intermediates is reached:

$$\mathrm{d[CpMn(ROCN)]}/\mathrm{d}t = k_1[\mathrm{CpMn}][\mathrm{ROCN}] - k_2[\mathrm{CpMn(ROCN)}][\mathrm{ROCN}] = 0$$

then

$$[\mathrm{CpMn(ROCN)}] = k_1[\mathrm{CpMn}]/k_2 \quad (9)$$

and

$$\mathrm{d[CpMn(ROCN)_2]}/\mathrm{d}t = k_2[\mathrm{CpMn(ROCN)}][\mathrm{ROCN}] - k_3[\mathrm{CpMn(ROCN)_2}][\mathrm{ROCN}] = 0$$

then, solving and substituting from equation (9):

$$[\mathrm{CpMn(ROCN)_2}] = k_2[\mathrm{CpMn(ROCN)}]/k_3 = k_1[\mathrm{CpMn}]/k_3 \quad (10)$$

So, equation (8) becomes, on substituting from equation (10):

$$-\mathrm{d[ROCN]}/\mathrm{d}t = k_1[\mathrm{CpMn}][\mathrm{ROCN}] \quad (11)$$

Replacing with $[\mathrm{ROCN}]/[\mathrm{ROCN}]_0 = x$, where $[\mathrm{ROCN}]_0$ is the initial cyanate functional group concentration, equation (11) can be written as

$$-\mathrm{d}x/\mathrm{d}t = k_1[\mathrm{CpMn}]x$$

This agrees well with the experimental results if x is replaced by the reactive fraction of the cyanate $(x - x_\infty)$ as defined before. CpMn represents the active catalyst after complete replacement of the carbonyl groups. This may be the pre-made catalyst or may be produced after direct irradiation.

It was considered in this mechanism that the 'active catalyst' was the CpMn species or other forms such as CpMn(CO). If this species coordinated with other compounds (e.g. H_2O) instead of cyanates, it would lose its activity. This could happen after a certain number of reaction cycles, which may explain the difference

between the limiting conversion values for different initial catalyst concentrations or different irradiated systems.

CONCLUSIONS

The kinetics of the thermal polymerization of Arocy B-10 catalysed by 1% of the organometallic compound tricarbonylcyclopentadienylmanganese has been investigated using d.s.c. and *FT*i.r.. The polymerization process included two stages: initial u.v. irradiation and thermal curing. The irradiation of the photocatalysts for 15–120 s lowered the cure temperature of the network by over 100°C. The resulting network had a T_g which was higher for the same extent of conversion than for the uncatalysed polymerization at higher temperature and was close to that expected from mean-field theory calculation of extent of conversion at gelation.

A model study of the photoproduct formed using a high cyanate *versus* Mn ratio supported the coordination between cyanate functional groups and the metal cation, but only a mixture of species could be obtained due to their high reactivities. The isolated photoproduct was an active catalyst for the cyclotrimerization.

The reaction rate was described by a first-order dependence on the active catalyst concentration and on the cyanate concentration. The activation energies for the different irradiated systems decreased slightly from 52 to 46 kJ mol^{-1} with the increase of irradiation time, and for the pre-made catalyst systems the value was about 67 kJ mol^{-1}. This activation energy difference may be explained by the different composition of active catalyst present in different systems.

A mechanism was proposed based on the kinetic data as well as the *FT*i.r. spectrum of the complex mixture formed in the model study. It involved the photosubstitution of the carbonyls in the original catalyst by the cyanate functional groups during the irradiation stage and the formation of the active catalyst species at the thermal curing stage. The proposed rate determining step was the addition of cyanate to a bisubstituted complex of $CpMn(CO)_3$ to form the triazine ring and to release the active catalyst CpMn or CpMn(CO).

REFERENCES

1 Hamerton, I. 'Chemistry and Technology of Cyanate Ester Resins', Blackie Academic & Professional, Glasgow, UK, 1994
2 Fyfe, C. A., Niu, J., Rettig, S. J., Burlinson, N. E., Reidsema, C. M., Wang, D. W. and Poliks, M. *Macromolecules* 1992, **25**, 6289
3 Osei-Owusu, A. and Martin, G. C. *Polym. Eng. Sci.* 1991, **31**, 1604
4 Shimp, D. A. *Am. Chem. Soc. Polym. Mater.: Sci. Eng.* 1986, **54**, 107
5 Bauer, M., Bauer, J. and Kuhn, G. *Acta Polym.* 1986, **37**, 715
6 Osei-Owusu, A. and Martin, G. C. *Polym. Eng. Sci.* 1992, **32**, 535
7 Zeng, S., Ahn, K. and Seferis, J. C. *Polym. Compos.* 1992, **13**, 191
8 Georjon, O., Galy, J. and Pascault, J. *J. Appl. Polym. Sci.* 1993, **49**, 1441
9 Simon, S. L. and Gillham, J. K. *J. Appl. Polym. Sci.* 1993, **47**, 461
10 Brownhill, A., Cunningham, I. D., Hamerton, I. and Howlin, B. J. *Am. Chem. Soc. Polym. Mater.: Sci. Eng.* 1994, **71**, 809
11 Meler, K. and Zwelfel, H. *J. Imaging Sci.* 1986, **30**, 174
12 McCormick, F. B., Brown-Wensley, K. A. and DeVoe, R. J. *Am. Chem. Soc. Polym. Mater.: Sci. Eng.* 1992, **66**, 460
13 Kotch, T. G. and Lees, A. J. *Am. Chem. Soc. Polym. Mater.: Sci. Eng.* 1992, **66**, 462
14 McCormick, R. B., Brown-Wensley, K. A. and DeVoe, R. J. *Eur. Patent Appl. 036 407 3A1*, 1989
15 Giiordano, P. J. and Wrighton, M. S. *Inorg. Chem.* 1977, **16**, 160
16 Lee, W. I., Loos, A. C. and Springer, G. C. *Compos. Mater.* 1982, **16**, 510
17 Krogmann, K. and Mattes, R. *Angew. Chem., Int. Edn.* 1966, **5**, 1046
18 Rybinskaya, M. I. and Korneva, L. M. *J. Organomet. Chem.* 1982, **231**, 25
19 Bland, W. J., Kemmitt, R. D. W. and Moore, R. D. *J. Chem. Soc., Dalton Trans.* 1973, 1292
20 Geoffroy, G. L. and Wrighton, M. S. 'Organometallic Photochemistry', Academic Press, New York, 1979, p. 131
21 Kutal, C. and Serpone, N. 'Photosensitive Metal–Organic Systems: Mechanistic Principles and Applications', American Chemical Society, Washington, DC, 1993, p. 50
22 Davies, S. D. 'Organotransition Metal Chemistry: Applications to Organic Synthesis', Pergamon Press, Oxford, UK, 1982, p. 225
23 Gill, T. P. and Mann, K. R. *Inorg. Chem.* 1980, **19**, 3007
24 Wisanrakkit, G. and Gillham, J. K. *Am. Chem. Soc. Polym. Mater.: Sci. Eng.* 1988, **59**, 969
25 Simon, S. L. and Gillham, J. K. *Am. Chem. Soc. Polym. Mater.: Sci. Eng.* 1989, **61**, 799
26 Gupta, A. M. *Macromolecules*, 1991, **24**, 3459
27 Fang, T. and Shimp, D. A. *Prog. Polym. Sci.* 1995, **20**, 84
28 Gupta, A. M. and Macosko, C. W. *Macromolecules* 1993, **26**, 2455